**IEEE Robotics and Automation Letters (RAL) paper presented at the**
**2020 IEEE/RSJ International Conference on Intelligent Robots and Systems (IROS)**
**October 25-29, 2020, Las Vegas, NV, USA (Virtual)**

# Stable Flight of a Flapping-wing Micro Air Vehicle Under Wind Disturbance

Jonggu Lee[1], Seungwan Ryu[1], and H. Jin Kim[1*]

***Abstract*— Flapping-wing micro air vehicles (FWMAVs) inspired by the nature are interesting flight platforms due to their efficiency, concealment and agility. However, most studies have been conducted in indoor environments where external disturbance is excluded because these FWMAVs are susceptible to disturbance due to their complex dynamics and small size. In order for these bio-inspired robots to perform various tasks outside, a capability to react robustly to external disturbance is essential. In this paper, we propose an algorithm that allows a FWMAV to fly well even under external disturbance. First, we derive the attitude dynamics of the FWMAV based on flight data. Then, we design a robust attitude controller using DOBC based on the dynamics. Also, we add a flight mode selector to recognize disturbance autonomously and switch to the robust control mode. Finally, we experiment outdoor flight of the FWMAV with wind disturbance. The FWMAV recognizes the existence of disturbance autonomously, and produces additional control inputs to compensate the disturbance. The proposed algorithm is validated with experiments.**


Fig. 1: Overlapped snapshots of a robotic bird flying in the presence of wind disturbance.

## I. INTRODUCTION

Recent years have seen a great interest in diverse forms of Micro Air Vehicles (MAVs) that can perform various tasks in a confined space. These MAVs usually operate in a low Reynolds number region because they are small in size and low in speed. In this region, it is known that the flapping-wing MAVs (FWMAVs) are more efficient than other flying vehicles and also able to achieve good maneuverability and agility [1]. Such advantages and pursuit of bio-inspiration have led to various experiments such as hovering [2], [3], tracking [4], [5], autonomous takeoff [6], obstacle avoidance [7], acrobatic movement [8] using FWMAVs. However, these experiments in common were conducted in an indoor environment where effects of disturbance such as wind are excluded. FWMAVs are susceptible to disturbance because they can only produce limited forces and moments due to their complex dynamics and small size. Despite the necessity to design a controller that can respond robustly to external disturbance, there are very few researches on this topic.

Researchers at Harvard university [9] tried to design an adaptive controller that can resist to wind disturbance with an insect-size FWMAV. The robot, lighter than 100 mg, has to be tethered for power and control, and the fragile nature of the robot restricts it from performing various missions. The authors acknowledge its limitation that the control strategy is based on debatable equations of force and moment generated by wind disturbance. Researchers at Purdue university [10] proposed a robust control algorithm that can detect the environmental changes such as grounds, walls or obstacles using the motor feedback data. The robot can fly even though it collides with obstacles, but it has to be tethered to external actuation and sensing devices. Also, the proposed algorithm has not been tested in windy environments.

One method to improve robustness is disturbance-observer-based control (DOBC). It estimates the disturbance or the influence of the disturbance, and makes an action to compensate the effect of the disturbance based on the estimation. It not only compensates external disturbance, but also model uncertainties such as unmodeled dynamics and parameter perturbation. Also, with DOBC, a nominal controller that is designed with classic control theory in the absence of disturbance can be used directly. All we have to do is to estimate the disturbance and add a feedforward control term in the inner loop of the nominal controller. By doing this, both the tracking performance and robustness can be achieved unlike most robust control theories such as $H-\infty$ control, where the nominal performance is sometimes sacrificed to obtain better robustness. Because of these advantages, DOBC has been successfully applied to various platforms, such as fixed-wing aircraft [11], rotary-wing aircraft [12], missile [13], aerial manipulator [14].

Although there have been many attempts to identify the dynamics of FWMAV in various ways, the exact phenomena caused by the flapping motion are not still well understood [15]. Also, complex fluid analysis is inevitable for precise modeling because the wings of FWMAV often consist of flexible thin-film. These problems make it very difficult to

This research was supported by a grant to Bio-Mimetic Robot Research Center Funded by Defense Acquisition Program Administration, and by Agency for Defense Development (UD190018ID).

[1]All authors are with the Department of Mechanical and Aerospace Engineering and Automation and System Research Institute (ASRI) at Seoul National University, Seoul, South Korea jonggu6986@gmail.com

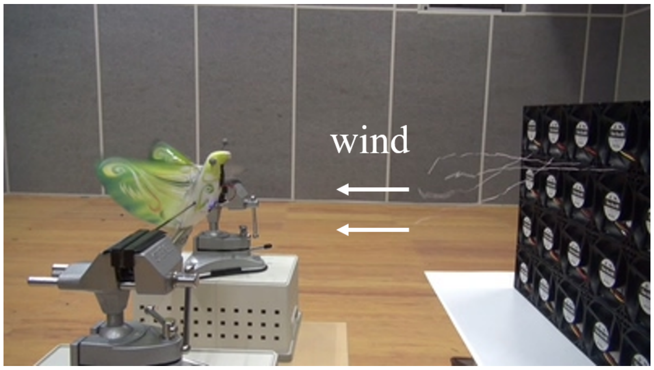


Fig. 2: Experimental setup for attitude dynamics modeling.

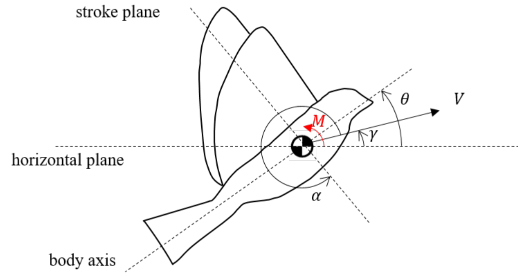


Fig. 3: Free body diagram of the robotic bird.

analyze forces and moments due to flapping motion, so many researchers who design and study FWMAVs assume simplified movements [16]. By applying DOBC to the FWMAV, the influence of this unmodeled dynamics could be minimized, and we can design a controller that can respond to external disturbance robustly.

In this paper, we propose an algorithm that allows the FWMAV to fly well even under external disturbance. First, we derive attitude dynamics of a FWMAV based on experimental data. In order to simulate flight of a FWMAV, we fix the robotic bird and generate a wind corresponding to the robotic bird's translational velocity in a laboratory condition to derive attitude dynamics of the FWMAV. Then we design a robust attitude controller using DOBC based on the dynamics. Also, we add a flight mode selector to recognize disturbance autonomously and switch to the robust control mode. The flight mode selector recognizes disturbance with anomaly detection algorithm based on sparse gaussian process regression. This algorithm does not assume the specific model of an aircraft, and applicable to various vehicles including FWMAV, unlike many previous anomaly detection algorithms [17], [18].

Most previous studies [2]–[7] usually design the controller assuming stable flight, and it is difficult to guarantee their flight performance when disturbance exists. There have been studies based on model-based robust control [10], [19]. However, their controller also is applicable only during stable maneuver, and only deals with model uncertainty. Also, the control input from the controller severely chatters and gets frequently saturated. There also have been attempts to achieve aggressive maneuver for a FWMAV. A predetermined feedforward control is used in [8] and deep learning is employed in [20]. But such approaches are applicable only to a limited set of prearranged tasks. This paper contains one of the first attempts to implement an algorithm that allows a palm-sized FWMAV to fly in a disturbance environment.

To validate our algorithm, we perform both tethered flight experiments and free flight experiments. In the tethered flight, to simulate a situation where the flying robotic bird encounters an external disturbance, we generate wind corresponding to the sum of the robotic bird's velocity and external wind disturbance to the tethered robotic bird. In the free flight, we apply wind disturbance to the actual platform. We can see that the robotic bird observes the disturbance and generates control inputs to maintain stable attitude by the proposed DOBC algorithm.

Our contributions are summarized as:

- Modeling of moments acting on a flying FWMAV
- Design of a robust controller for a FWMAV to maintain stable attitude
- Anomaly (disturbance) detection algorithm generally applicable to various vehicles including FWMAV
- Application of the proposed algorithm to a flying bird and performance validation

The rest of the paper is organized as follows. In Section II, we cover the attitude dynamics model of the robotic bird. Based on experimental data, we propose a simple model describing the moments that occur when the robotic bird is flying. In Section III, we propose a robust control algorithm to deal with unknown external disturbance and model uncertainty, and find a disturbance situation. The results of experiments are displayed in Section IV. Section V concludes the paper.

## II. MODELING ATTITUDE DYNAMICS

The FWMAV used in this paper is shown in Figure 2, and the detailed descriptions of the robotic bird can be found in our previous work [4]. It has two pairs of flapping wings and a rudder in the tail wing. For weight consideration, there is no onboard device other than the actuators and transceiver. In this section, we derive the data-driven longitudinal attitude dynamics of the robotic bird.

Various studies have been conducted on the longitudinal movement of the FWMAV [21]–[23]. In tailed FWMAVs, the tail wing provides internal stability in a cruise condition, i.e., when a small perturbation in a equilibrium state causes the robot to vibrate in the pitch direction, and the tail wing can dampen this vibration passively. However, if the gust blows and the robot loses its attitude, this vibration can become so big that it is difficult to restore the flight performance by the passive damping of the tail wing only. The robot controls the flapping frequency through robust control based on the model in this section so that the robot can recover from such perturbation.

The flapping wing has three independent rotational movements around the body: flapping motion around the body axis, feathering motion around the axis of the wing, and deviation motion up and down on the plane of the wing. But it is difficult to consider all these rotational movements, and experimental data shows that flapping motion is the most dominant motion in our platform. In this paper, we only consider the effects of flapping motion. Also, all dynamics in this paper is cycle-averaged.

The free body diagram of the robotic bird in flight is shown in Figure 3. In this paper, we use ZXY-Euler angle sequence to avoid singularities since our robotic bird operates at high pitch angles in disturbance region. $V$ is the velocity of the robotic bird, $\theta$ is the pitch angle, $\gamma$ is the flight path angle, and $\alpha$ is the stroke plane angle defined by the angle between the velocity and the stroke plane. We assume free forward flight ($\gamma \approx 0$) and $\alpha$ can be calculated by

$$\alpha = \theta - \pi/2 \tag{1}$$

When the robotic bird is flying, we assume that the moments applied to the bird can be classified into four:

- moment generated by the flapping motion itself, $M_1$
- moment generated by the translational motion like fixed-wing aircraft, $M_2$
- moment generated by collaborative effects of both translation motion and flapping motion, $M_3$
- moment generated by natural damping induced by angular motion, $M_4$

These moments can be parameterized as follows:

$$\begin{aligned} M_1 &= f_1(\omega) \\ M_2 &= f_2(V,\alpha) = \frac{1}{2}\rho V^2 C_m(\alpha) Sc \\ M_3 &= f_3(V,\omega) \\ M_4 &= f_4(\dot{\theta}) \end{aligned} \tag{2}$$

where $\omega$ is the flapping frequency, $\rho$ is the density of air, $C_m$ is the pitching moment coefficient of the robotic bird and it is a nonlinear function of $\alpha$, $S$ is the area of the wing, and $c$ is the chord length of the wing. We model each of the moments $M_1, M_2, M_3, M_4$ based on experimental data as described below. We treat the robotic bird as a black box with the data-driven modeling process which can cause modeling error, but the robust controller to be described in Sec III-B can stabilize the system even with this data-driven model. Physical models of other FWMAV can be found in [24], [25].

### A. Modeling without translational motion

First, we model the moments $M_1$ and $M_4$ in the absence of translational movement of robotic bird (i.e. $V = 0$). As shown in Figure 2, we fix the robotic bird so that it could rotate in pitch direction only. The axis of rotation is set to pass through the center of gravity of the robotic bird to eliminate the gravitational effects. We apply random control signals generated by a human to the robotic bird through the RC controller. Then the robotic bird rotates around the center of gravity point (tethered axis), and we collect the pitch angle and flapping frequency data with a motion capture system for 10 minutes. Acceleration and velocity information is estimated from Kalman filter [26] The attitude dynamics of the robotic bird when there is no translational motion is as follows, where $I$ is the moment of inertia of the robotic bird, and it is a known constant.

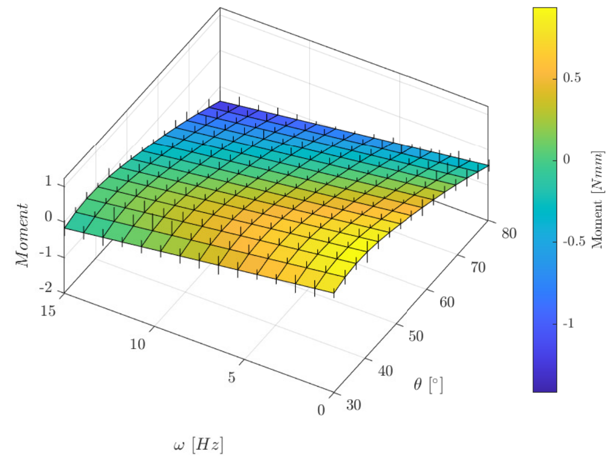


Fig. 4: Optimized attitude dynamics model when the robotic bird moves at a speed of $V = 1.4$ m/s and $\dot{\theta} = 0$

$$I\ddot{\theta} = M_1 + M_4 \tag{3}$$

Based on the above training data, we can estimate the moments $M_1$ and $M_4$ minimizing the following loss function $L_1$. We assume that the moment due to the flapping itself $M_1$ is proportional to the flapping frequency and $M_4$ is proportional to the pitch rate. In fact, the force and moment due to flapping motion is quadratic to the flapping frequency [27]. However, even if the moment is treated to be linearly proportional to the flapping frequency, the regression is effective enough practically [28]. The weighted least square (WLS) method is used for optimization.

$$\begin{aligned} L_1 &= I\ddot{\theta} - (M_1 + M_4) \\ M_1 &= k_1\omega \\ M_4 &= k_4\dot{\theta} \end{aligned} \tag{4}$$

where $k_1$, $k_4$ are constants to be optimized.

### B. Modeling with translational motion

In this subsection, we model moments generated by translational motion. The basic data collection setup is same as in Section II-A. In addition to the previous setup, we add a multiple-fan wind tunnel to make the free stream velocity as if the robotic bird is flying in the air. The wind generator consists of an array of twenty 12V DC fans and its dimension is $40 \times 32$ cm. An arduino board controls the speed of wind by pulse-width modulation (PWM) singal between 0 and 4.8 m/s. The tested free stream velocities range from 0.5 m/s to 2 m/s, with an increment of 0.3 m/s. In the same way as Section II-A, we measure the pitch angle and flapping frequency for every 10 minutes. The attitude dynamics of the robotic bird with translational motion is as follows.

$$I\ddot{\theta} = M_1 + M_2 + M_3 + M_4 \tag{5}$$

We can model $M_2$ and $M_3$ so that the loss function $L_2$ defined below is minimized using the dynamic parameters calculated in Section II-A. We model $C_m$ as a $N$-th order fourier series because it is a periodic function with period $2\pi$. $M_3$ is assumed to be proportional to the flapping frequency $\omega$ and proportional to the square of free stream velocity $V$ with our heuristic knowledge. WLS is used for optimization as before.

$$\begin{aligned}
L_2 &= (I\ddot{\theta} - M_1 - M_4) - (M_2 + M_3) \\
C_m(\alpha) &= \sum_{n=0}^{N} (a_n sin(n\alpha) + b_n cos(n\alpha)) \\
M_2 &= \frac{1}{2}\rho V^2 C_m(\alpha) Sc \\
M_3 &= k_3 V^2 \omega
\end{aligned} \tag{6}$$

where $a_n$, $b_n$, $k_3$ are constants to be optimized. The overall optimized results in Section II are shown in Figure 4, where a vertical bar at each point represents the $\pm\sigma$ interval.

## III. ROBUST CONTROL ALGORITHM

We use the disturbance-observer-based controller (DOBC) [29] for robust attitude control of a FWMAV. From Section II, the attitude dynamics of the robotic bird with velocity $V$ is represented as follows.

$$\ddot{\theta} = F(\theta, \dot{\theta}, \omega, V) \tag{7}$$

The velocity of our robotic bird does not change significantly in cruise condition, so we treat the velocity $V$ as a constant. Then, the attitude dynamics can be considered as a nonlinear system whose state is $\theta$ and control is $\omega$. We design a robust controller of the FWMAV that can maintain stable attitude in spite of external disturbance based on the DOBC. Also, we design a flight mode selector to recognize disturbance and switch to the robust control mode.

### A. Nominal controller

Before designing a disturbance observer and compensator, we design two nominal controllers. The nominal controllers are designed with assumption that there is no external disturbance and model uncertainty. One is the controller for tethered flight, and it is designed to maintain a desired pitch angle. The other is the controller for free flight, and it is designed to follow the desired path.

*1) Tethered flight:* We use model predictive control (MPC) to maintain a desired pitch angle. The following optimization problem is solved with iLQR [30].

$$\begin{aligned}
\Omega &= \arg\min \sum_{i=0}^{H} c(\theta_i, \dot{\theta}_i, \omega_i) \\
\text{subject to } \ddot{\theta}_i &= F(\theta_i, \dot{\theta}_i, \omega_i, V)
\end{aligned} \tag{8}$$

where $\Omega$ is a sequence of the optimal flapping frequency, $H$ is the MPC time horizon, and the subscript $i$ denotes the value at the $i$-th time step. The cost function $c(\theta, \dot{\theta}, \omega)$ is

$$c(\theta, \dot{\theta}, \omega) = k_\theta(\theta - \theta_r)^2 + k_{\dot{\theta}}\dot{\theta}^2 + k_\omega(\omega - \omega_r)^2 \tag{9}$$

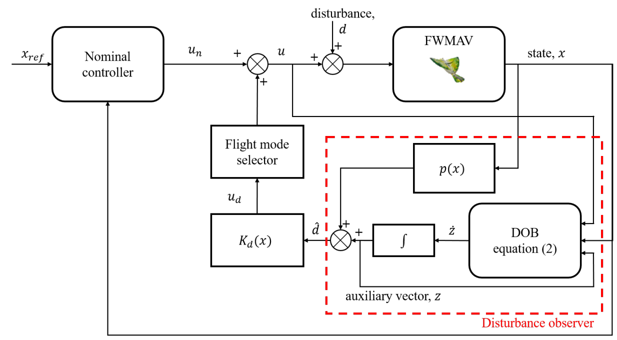


Fig. 5: Block diagram of the proposed DOBC method for the FWMAV with nonlinear dynamics.

where $k_\theta, k_{\dot{\theta}}, k_\omega$ are the weight factors for each cost term, $\theta_r$ is the desired pitch angle, and $\omega_r$ is the equilibrium flapping frequency corresponding to the given desired pitch angle $\theta_r$, i.e.,

$$0 = F(\theta_r, 0, \omega_r, V) \tag{10}$$

When we obtain the optimal sequence of flapping frequency $\Omega$ by the above optimization process, only the first component of $\Omega$ is used as a control input. Then, the optimal frequency sequence is recalculated at the next time step and this process is repeated.

*2) Free flight:* We use a simple PID controller to follow the desired path. Longitudinal control is achieved by the flapping motion, and the lateral control is achieved by the rudder. The gains of the controllers are experimentally tuned.

### B. Disturbance and uncertainty compensator

Here, we design a robust controller based on DOBC to maintain the desired attitude. The dynamics (7) can be expressed in the following form:

$$\begin{aligned}
\dot{x} &= f(x) + g_1(x)u + g_2(x)d \\
y &= h(x)
\end{aligned} \tag{11}$$

where $x = [\theta, \dot{\theta}]^T$, $u = \omega$, $d \in R^2$, $y = \theta$ denote the state, input, disturbance and output vectors, respectively. $f(x)$, $g_1(x)$ and $g_2(x)$ are smooth functions in terms of state $x$. We can design the following disturbance observer for this system to estimate the unknown disturbance $d$ [29].

$$\begin{aligned}
\dot{z} &= -\frac{\partial p}{\partial x}(x)g_2(x)z - \frac{\partial p}{\partial x}(x)(f(x) + g_1(x)u + g_2(x)p(x)) \\
\hat{d} &= z + p(x)
\end{aligned} \tag{12}$$

where $\hat{d}$ is the estimated disturbance, $z$ is an auxiliary vector and $p(x)$ is the observer gain function to be designed. The disturbance estimation error is defined as

$$e_d = \hat{d} - d \tag{13}$$

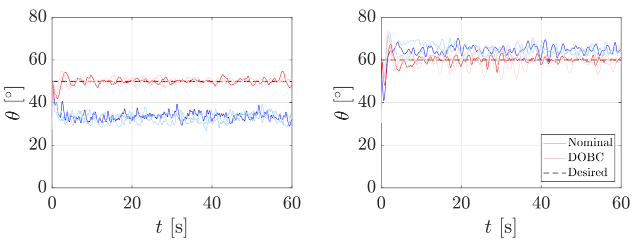


(a) $\theta_r = 50°$ (b) $\theta_r = 60°$

Fig. 6: Results from the tethered flight experiments of the robotic bird with translational velocity $V$. Light-colored lines are individual flight trajectories and thick solid-colored lines are representative trajectories.

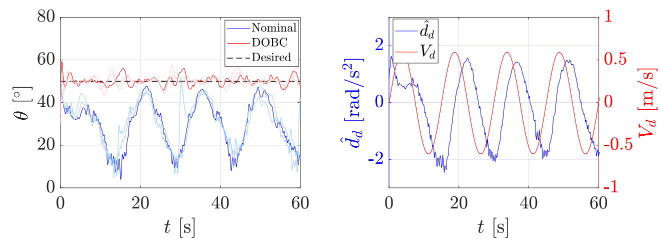


(a) $\theta_r = 50$ (b) $\hat{d}_d$

Fig. 7: Results from the tethered flight experiments of the robotic bird with translational velocity $V$, when there is unknown wind disturbance $V_d$. (a) Attitude trajectories. (b) Estimation results of pure external disturbance on the angular velocity channel and the corresponding wind disturbance.

Combining the system dynamics (11), disturbance observer (12), and error (13) yields

$$\begin{aligned} \dot{e}_d &= \dot{\hat{d}} - \dot{d} = \dot{z} + \dot{p}(x) - \dot{d} \\ &= -\frac{\partial p}{\partial x}(x) g_2(x) e_d - \dot{d} \end{aligned} \tag{14}$$

This system is asymptotically stable under the assumption that the disturbance $d$ varies slowly compared to the observer dynamics ($\dot{d} \approx 0$) and if we select $p(x)$ properly. Then, the estimated disturbance from the disturbance observer can follow the actual disturbance. The disturbance-observer-based control law is proposed to compensate the effect of disturbance as

$$\begin{aligned} u &= u_n + u_d \\ &= u_n + K_d \hat{d} \end{aligned} \tag{15}$$

where $u$ is the total control input, $u_n$ is the control input from the nominal controller in Section III-A, $K_d$ is the disturbance compensation gain. The details of calculation of $K_d$ and the stability analysis are in [29].

### C. Flight mode selector

We design two flight modes. One is the nominal mode where the nominal controller operates. With DOBC, it is inevitable to sacrifice the altitude maintenance performance during flight. Therefore, when there is no disturbance, only the nominal controller operates to achieve the maximum tracking performance. The other is the robust control mode, which prioritizes a stable attitude to avoid falling, losing some tracking accuracy. DOBC is used in the robust control mode. Despite we set the desired angle in DOBC as the attitude value in the cruise condition of the robotic bird to regulate the altitude, the tracking accuracy must be sacrificed. This mode is only activated when disturbance exists to maximize the tracking performance. This approach provides the ability that the FWMAV maximizes the tracking performance while flies robustly in response to disturbance.

To determine which flight mode to use during the flight, we add a flight mode selector that checks the existence of the disturbance. It is implemented through sparse gaussian process regression (GPR). This flight mode selector is designed as follows.

We collect flight trajectory of FWMAV $\tau = (\mathbf{s}_0, \mathbf{a}_0, \cdots, \mathbf{s}_{T-2}, \mathbf{a}_{T-2}, \mathbf{s}_{T-1})$ of length $T$ in the disturbance-free environment. The state vector $\mathbf{s}_t = \left[\boldsymbol{\theta}^T, \boldsymbol{v}^T, \boldsymbol{\omega}^T\right]^T$ includes the euler angle, body velocity, body angular velocity of FWMAV, and the action $\mathbf{a}_t$ is control signal of actuators. We parameterize our nominal dynamics function $\hat{f}(s_t, a_t) = (s_{t+1} - s_t)$ as GPR off-line. Then, we can predict the mean $m$ and variance $\mu$ of next state $s_{t+1}$ with this GPR on-line. If the Z-score during the flight $Z = (s_{t+1} - m(s_t, a_t))/\mu(s_t, a_t)$ is bigger than the threshold $T$, it is determined that there is disturbance and DOBC is turned on. We use the threshold of Z-score as 4, which corresponds to the 99.994% confidence interval.

The total control structure of the proposed algorithm is shown in Figure 5. In the nominal mode, only the nominal controller operates and the robotic bird follows the desired path (free flight case). However, when there is a disturbance, our flight mode selector recognizes it and activates the robust control mode. In this mode, the inner loop of DOBC compensates both model uncertainty and external disturbance, and the control input is generated to maintain the stable attitude and make a stable flight.

## IV. Experiment

We validate the proposed algorithm through experiments. The experimental setup is illustrated in Figures 1 and 2. The MPC time horizon $H$ is set to 60, and the sampling time $\Delta t$ is 0.01 second. The control system is implemented on a laptop computer with an Intel Core i7-8550U CPU running at 4.0 GHz. Motion capture camera was used to measure the flight states of the bird.

| | $\boldsymbol{\theta_r}$(°) | **Nominal**(°) | **DOBC**(°) |
|---|---|---|---|
| **Experiment A** | 60 | 5.4355 | 3.8162 |
| | 50 | 17.2901 | 2.0522 |
| **Experiment B** | 50 | 22.7178 | 2.6822 |

TABLE I: RMS error with the nominal controller and DOBC

### A. *Tethered flight*

*1) Experiment without external disturbance:* The first set of experiments aims to maintain a desired pitch angle while the robotic bird flies at the constant velocity of $V = 1.4$ m/s. The test setup was devised to imitate such condition in an indoor laboratory by fixing the robotic bird and blowing a constant wind $V_{wind} = V$ using the wind generator. The corresponding experiment results are presented in Figure 6. To analyze the effect of model uncertainty, two different desired pitch angles $\theta_r$ were selected. Six flights were performed with the nominal model-based control and the disturbance-observer-based control at each desired pitch angle.

It is difficult to model accurately the complicated movements of the flapping, and there exists modeling error. In our setup, the more stable pitch angle is, the more amount of regression data are collected in Section II. Therefore, as the pitch angle is close to the unstable region (low pitch), the model accuracy decreases. We notice the performance of the nominal controller when the desired pitch angle $\theta_r = 50^\circ$ is poor than $\theta_r = 60^\circ$. On the other hand, with DOBC, we can compensate this model uncertainty and follow the desired pitch angle regardless of the value.

*2) Experiment with external disturbance:* In the second experiment, unknown wind disturbance is added to the previous experiment. To test the robustness against the disturbance, wind with velocity $V_{wind} = V + V_d$ is blown from the wind generator, where the unknown time-varying wind disturbance $V_d$ is designed as

$$V_d = A \sin\left(\frac{2\pi}{T} t\right) \tag{16}$$

where $A = 0.6$ m/s is the amplitude of disturbance and the $T = 15$ s is the period of disturbance. Six flights were performed with each controller.

The corresponding flight trajectories are shown in Figure 7a. Despite the sinusoidal disturbance, the DOBC follows the desired trajectory just like the previous results in Section IV-A.1, while the nominal controller shows oscillation according to the velocity of wind.

In Section IV-A.1 we estimate and compensate the influence of model uncertainty $\hat{d}_m$, and we estimate and compensate the influence of both model uncertainty and external disturbance $\hat{d}$ in Section IV-A.2. With these two results, we can measure the influence of the pure external disturbance, $\hat{d}_d$. The effect of pure disturbance is the influence of both model uncertainty and external disturbance minus the average effect of model uncertainty:

$$\hat{d}_d = \hat{d} - \frac{1}{|D|} \sum_{\hat{d}_m \in D} \hat{d}_m \tag{17}$$

where $D$ is the dataset obtained in Section IV-A.1. Time histories of the influence of the pure disturbance $\hat{d}_d$ and the external wind disturbance $V_d$ are shown in Figure 7b. We can check that our estimated disturbance $\hat{d}_d$ follows the $V_d$ with a small time delay. Such time delay is explained by two reasons. One is the slow multiple-fan dynamics. $V_d$ is the command to the fans, and the actual wind disturbance has the latency because of the actuator delay and the distance between the robotic bird and the multiple-fan. Also, we design a low-pass filter to estimate the disturbance on-line, and there is an associated delay.

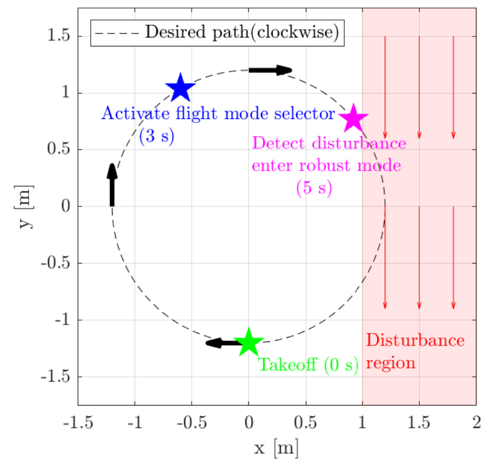


Fig. 8: Overview of the free flight experiments.

As the external disturbance $V_d$ becomes more powerful, its influence on the attitude dynamics of the robot will increase, and the actual estimation results from DOBC match our physical insight. Also, the Figure 7 and Table I confirm that the proposed control can estimate and compensate external disturbance and model uncertainty well, and significantly reduce the RMS error.

### B. *Free flight*

After the tethered flight experiments, we perform free flight experiments. An overview of the experiment is shown in Figure 8. First, the robotic bird takes off in a disturbance-free region, and it enters the disturbance region. In the disturbance region, the center of the wind fan with a diameter of 1 m is located at $(x, y) = (1.5, 2)$ and it generates a constant wind of 2 m/s. Such wind speed is equivalent to 150% of the equilibrium speed of the robotic bird, and especially given that our robot weighs only 16 grams, the 2 m/s wind is very strong. When the robot enters the wind region, the wind causes a severe pitch-down motion which makes the robot to oscillate in the pitch direction. With DOBC, the robot regulates this oscillation and restores the flight performance. Ten flights were performed with each controller.

In the equilibrium state (i.e. no-disturbance region), the tail wing regulates pitch angle passively, and the attitude control is less important than the altitude. In order to maintain desired altitude, the robotic bird adjust flapping frequency with the PID controller described in Section III-A.2. On the other hand, in the disturbance region, maintaining the stable attitude is more important than path following, so the DOBC controller is designed to maintain the equilibrium pitch angle, not the altitude. Because there is the trade-off between the control performances in altitude vs. attitude, the flight mode selector is used to determine which control mode should be employed.

At the beginning of the flight, there is no disturbance and the robotic bird is in the contact with another object (e.g. hand or launcher) for takeoff, and its dynamics is very different from the attitude dynamics derived in Section II. Therefore, the flight mode selector is not activated immediately after takeoff, and the bird is on nominal mode. Also, the control input of DOBC $u_d$ is not applied to the robotic bird, but the state variables used in DOBC such as $z$, $\hat{d}$ are being updated internally for fast adaptation.

A few seconds after takeoff, the robot activates the flight mode selector. Anomaly detection results of the flight mode selector during free flight are shown in Figure 9. The robotic bird enters the disturbance region x $>$ 1 m at 5 seconds. After about 0.2 seconds, the Z-score of the flight mode selector exceeds the anomaly threshold because the flight trajectories of the robotic bird are beyond the previously learned stable flight trajectories due to the disturbance. Then, our robot detects danger and enters the robust control mode to ensure the flight stability. In the early stage of the robust control mode, the Z-score is slightly larger than the stable flight due to disturbance. However, after 8 seconds, our DOBC regulates the flight attitude and the Z-score is reduced to the level similar to before entering the disturbance region. It is shown in Figure 9a. On the other hand, with only the nominal controller, the robot loses flight stability and becomes out of control, so it cannot reduce the Z-score. Finally, the robot crashes to the ground. It is shown in Figure 9b.

The attitude trajectories of free flight are shown in Figure 10. When entering the disturbance region at 5 seconds, the disturbance causes the pitch-down motion of the robotic bird. In Figure 4, the pitch-down motion produces a pitch-up moment, which generates a pitch-down moment again. Therefore, the robotic bird oscillates in the pitch direction, which should be regulated for stability. When we use only the nominal controller, the robotic bird oscillates aggressively and finally it loses stability and crashes. On the other hand, DOBC helps the robotic bird to maintain the stable attitude, and it can fly even in the disturbance region.

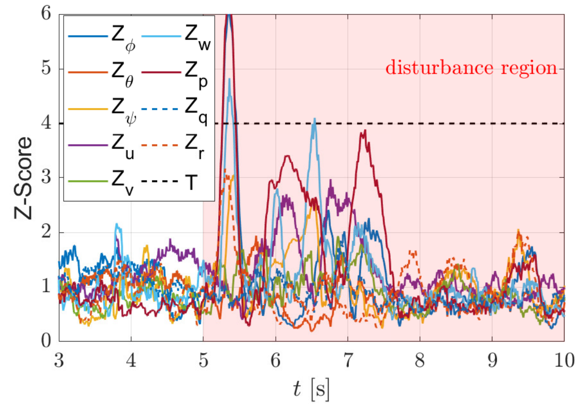


(a) Proposed control algorithm

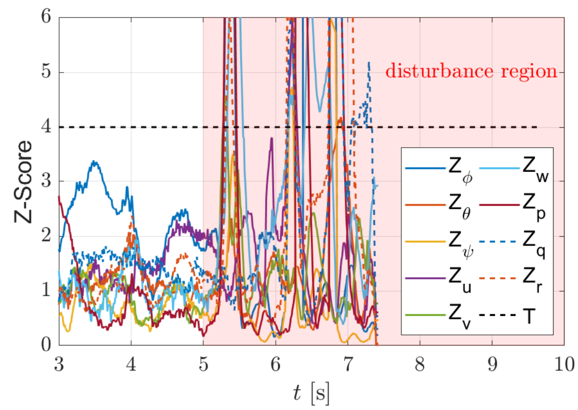


(b) Nominal control algorithm

Fig. 9: Anomaly detection results of flight mode selector during free flight. When the Z-score is larger than the threshold $T$, the robot detects disturbance and switches to the robust flight mode. (a) With the proposed control algorithm, the robot can stabilize its attitude, and the Z-score is reduced despite the disturbance. (b) With nominal control algorithm, the robot becomes out of control due to the disturbance, and the Z-score in disturbance region fluctuates widely.

## V. CONCLUSIONS

This paper proposes one of the first attempts to design an algorithm that allows a palm-sized FWMAV to fly in a disturbance environment. We build a simplified attitude dynamics model of a FWMAV based on experimental flight data. With this dynamics, we construct a robust attitude controller for a FWMAV using a disturbance observer. Unlike the previous studies on disturbance rejection of a FWMAV, we estimate the effects of disturbance based on the actual plant behavior, without a debatable explicit equation of wind disturbance. Also, to determine when to perform robust control, we add an anomaly detection algorithm using GPR. With our flight mode selector, the robotic bird detects disturbance and selects flight mode. The proposed anomaly detection algorithm is based on supervised learning. Therefore, if an appropriate input-output dataset of the aircraft can be obtained, the proposed algorithm can be generally applied to various platforms, unlike the existing anomaly detection algorithm. The proposed robust control algorithm is validated in the flight control experiments.

We use a multiple-fan wind tunnel to determine the attitude dynamics of a FWMAV. Although there is some modeling error due to the assumption in the moments of flying robotics bird, we can regulate the attitude of the FWMAV with DOBC even under the external disturbance. Also, with proposed anomaly detection algorithm, we are able to specify when the disturbance affects the flight performance during the flight. When the disturbance is detected, the robotic bird changes the flight mode to ensure stable flight, and can fly stably with robust control. It is expected that this research will contribute to the development of FWMAVs which can perform various outdoor missions.

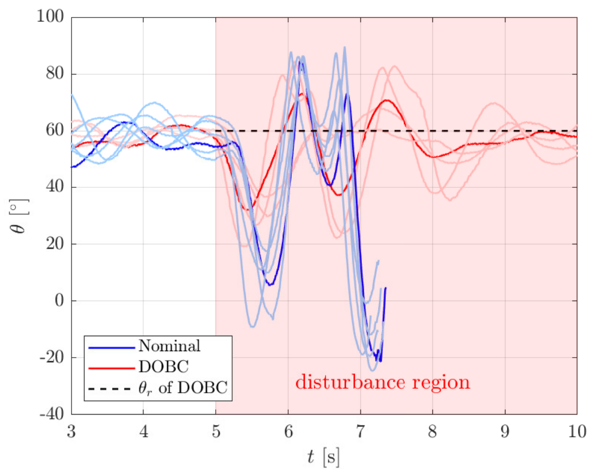


Fig. 10: Results from the free flight experiments. Light-colored lines are individual flight trajectories and thick solid-colored lines are representative trajectories. At 5 seconds, the robot enters the disturbance region and our flight mode selector recognizes it. With the proposed algorithm, the robot can stabilize its attitude even under wind disturbance, unlike the nominal algorithm.

## REFERENCES

[1] U. Pesavento and Z. J. Wang, "Flapping wing flight can save aerodynamic power compared to steady flight," *Physical review letters*, vol. 103, no. 11, p. 118102, 2009.

[2] J. Verboom, S. Tijmons, C. De Wagter, B. Remes, R. Babuska, and G. C. de Croon, "Attitude and altitude estimation and control on board a flapping wing micro air vehicle," in *2015 IEEE International Conference on Robotics and Automation (ICRA)*. IEEE, 2015, pp. 5846–5851.

[3] S. Ryu and H. J. Kim, "Development of a flapping-wing micro air vehicle capable of autonomous hovering with onboard measurements," in *2017 IEEE/RSJ International Conference on Intelligent Robots and Systems (IROS)*. IEEE, 2017, pp. 3239–3245.

[4] J. Lee, S. Ryu, T. Kim, W. Kim, and H. J. Kim, "Learning-based path tracking control of a flapping-wing micro air vehicle," in *2018 IEEE/RSJ International Conference on Intelligent Robots and Systems (IROS)*. IEEE, 2018, pp. 7096–7102.

[5] S. S. Baek, F. L. G. Bermudez, and R. S. Fearing, "Flight control for target seeking by 13 gram ornithopter," in *2011 IEEE/RSJ International Conference on Intelligent Robots and Systems*. IEEE, 2011, pp. 2674–2681.

[6] C. J. Rose, P. Mahmoudieh, and R. S. Fearing, "Coordinated launching of an ornithopter with a hexapedal robot," in *2015 IEEE International Conference on Robotics and Automation (ICRA)*. IEEE, 2015, pp. 4029–4035.

[7] C. De Wagter, S. Tijmons, B. D. Remes, and G. C. de Croon, "Autonomous flight of a 20-gram flapping wing mav with a 4-gram onboard stereo vision system," in *2014 IEEE International Conference on Robotics and Automation (ICRA)*. IEEE, 2014, pp. 4982–4987.

[8] M. Karásek, F. T. Muijres, C. De Wagter, B. D. Remes, and G. C. de Croon, "A tailless aerial robotic flapper reveals that flies use torque coupling in rapid banked turns," *Science*, vol. 361, no. 6407, pp. 1089–1094, 2018.

[9] P. Chirarattananon, K. Y. Ma, R. Cheng, and R. J. Wood, "Wind disturbance rejection for an insect-scale flapping-wing robot," in *2015 IEEE/RSJ International Conference on Intelligent Robots and Systems (IROS)*. IEEE, 2015, pp. 60–67.

[10] Z. Tu, F. Fei, J. Zhang, and X. Deng, "Acting is seeing: Navigating tight space using flapping wings," in *2019 International Conference on Robotics and Automation (ICRA)*. IEEE, 2019, pp. 95–101.

[11] S. J. Lee, K. E. Hashemi, M. C. Drew, N. T. Nguyen, and H. J. Kim, "Robust gust load alleviation control using disturbance observer for generic flexible wing aircraft in cruising condition," in *2018 Annual American Control Conference (ACC)*. IEEE, 2018, pp. 2257–2263.

[12] C. Liu, W.-H. Chen, and J. Andrews, "Tracking control of small-scale helicopters using explicit nonlinear mpc augmented with disturbance observers," *Control Engineering Practice*, vol. 20, no. 3, pp. 258–268, 2012.

[13] W.-H. Chen, "Nonlinear disturbance observer-enhanced dynamic inversion control of missiles," *Journal of Guidance, Control, and Dynamics*, vol. 26, no. 1, pp. 161–166, 2003.

[14] S. Kim, S. Choi, H. Kim, J. Shin, H. Shim, and H. J. Kim, "Robust control of an equipment-added multirotor using disturbance observer," *IEEE Transactions on Control Systems Technology*, vol. 26, no. 4, pp. 1524–1531, 2018.

[15] W. Shyy, Y. Lian, J. Tang, D. Vieiru, and H. Liu, *Aerodynamics of low Reynolds number flyers*. Cambridge University Press, 2007, vol. 22.

[16] C. T. Orlowski and A. R. Girard, "Modeling and simulation of nonlinear dynamics of flapping wing micro air vehicles," *AIAA journal*, vol. 49, no. 5, pp. 969–981, 2011.

[17] W. Han, Z. Wang, and Y. Shen, "Fault estimation for a quadrotor unmanned aerial vehicle by integrating the parity space approach with recursive least squares," *Proceedings of the Institution of Mechanical Engineers, Part G: Journal of Aerospace Engineering*, vol. 232, no. 4, pp. 783–796, 2018.

[18] X. Qi, D. Theilliol, J. Qi, Y. Zhang, and J. Han, "A literature review on fault diagnosis methods for manned and unmanned helicopters," in *2013 International Conference on Unmanned Aircraft Systems (ICUAS)*. IEEE, 2013, pp. 1114–1118.

[19] J. Zhang, B. Cheng, and X. Deng, "Instantaneous wing kinematics tracking and force control of a high-frequency flapping wing insect mav," *Journal of Micro-Bio Robotics*, vol. 11, no. 1-4, pp. 67–84, 2016.

[20] F. Fei, Z. Tu, J. Zhang, and X. Deng, "Learning extreme hummingbird maneuvers on flapping wing robots," in *2019 International Conference on Robotics and Automation (ICRA)*. IEEE, 2019, pp. 109–115.

[21] I. Faruque and J. S. Humbert, "Dipteran insect flight dynamics. part 1 longitudinal motion about hover," *Journal of theoretical biology*, vol. 264, no. 2, pp. 538–552, 2010.

[22] Y. Xiong and M. Sun, "Dynamic flight stability of a bumblebee in forward flight," *Acta Mechanica Sinica*, vol. 24, no. 1, pp. 25–36, 2008.

[23] J. M. Dietl and E. Garcia, "Stability in ornithopter longitudinal flight dynamics," *Journal of Guidance, Control, and Dynamics*, vol. 31, no. 4, pp. 1157–1163, 2008.

[24] H. E. Taha, M. R. Hajj, and A. H. Nayfeh, "Longitudinal flight dynamics of hovering mavs/insects," *Journal of Guidance, Control, and Dynamics*, vol. 37, no. 3, pp. 970–979, 2014.

[25] H. E. Taha, S. Tahmasian, C. A. Woolsey, A. H. Nayfeh, and M. R. Hajj, "The need for higher-order averaging in the stability analysis of hovering, flapping-wing flight," *Bioinspiration & biomimetics*, vol. 10, no. 1, p. 016002, 2015.

[26] G. Bishop and G. Welch, "An introduction to the kalman filter," *Proc of SIGGRAPH 2001, Course 8 (27599-23175) : 41*, 2001.

[27] S. Ansari, R. Żbikowski, and K. Knowles, "Aerodynamic modelling of insect-like flapping flight for micro air vehicles," *Progress in Aerospace Sciences*, vol. 42, no. 2, pp. 129–172, 2006.

[28] M. Karasek, A. Hua, Y. Nan, M. Lalami, and A. Preumont, "Pitch and roll control mechanism for a hovering flapping wing mav," *International Journal of Micro Air Vehicles*, vol. 6, no. 4, pp. 253–264, 2014.

[29] J. Yang, W.-H. Chen, and S. Li, "Non-linear disturbance observer-based robust control for systems with mismatched disturbances/uncertainties," *IET control theory & applications*, vol. 5, no. 18, pp. 2053–2062, 2011.

[30] D. Mayne, "A second-order gradient method for determining optimal trajectories of non-linear discrete-time systems," *International Journal of Control*, vol. 3, no. 1, pp. 85–95, 1966.